Arch. Metall. Mater. **65** (2020), 1, 433-440

DOI: 10.24425/amm.2020.131746

XU JIA NING[1], YANG HONG YING[1*], TONG LIN LIN[1]

ADSORPTION BEHAVIOR OF GLUCURONIC ACID ON PYRITE SURFACE: AN ELECTROCHEMICAL AND DFT STUDY

Bacterial adsorption on mineral surface is one of the key steps in bioleaching process. The bacteria adsorb on the mineral surface via the extracellular polymeric substances (EPS) layer. In this paper, the behavior of glucuronic acid, one of the key substances in EPS layer, adsorbed on the pyrite surface is studied using DFT and electrochemical methods. Adsorption capacity of glucuronic acid is stronger than that of water. Glucuronic acid adsorbs on pyrite surfaces and it follows a mixed type of interactions (physisorption and chemisorption). Adsorption of glucuronic acid on pyrite surface followed Langmuir's adsorption isotherm with adsorption standard free energy of –27.67kJ mol^{-1}. The structural and electronic parameters were calculated and discussed.

Keywords: glucuronic acid, pyrite, adsorption

1. Introduction

Bioleaching is an environmentally friendly and economically feasible technology [1,2]. In bioleaching process bacteria oxidize Fe^{2+} and enrich Fe^{3+} on the surface of minerals, consequently, accelerating the dissolution of minerals [3-5]. Bioleaching technology is often used to recover gold [6], copper [7], zinc [8] and other metals. Pyrite is the most widely distributed sulfide mineral in nature and is often associated with gold [9], copper [10] and zinc minerals [11]. In the bioleaching process, pyrite plays an important role in the leaching of other minerals, including the formation of galvanic cells with other minerals [12,13], encapsulation of other minerals [14,15], etc. Therefore, bioleaching of pyrite has attracted widely attention [5,6,8,9,12, 3].

In recent years, a consensus has been gradually reached on the mechanism of bioleaching pyrite: bacteria can not directly dissolve pyrite. In the process of bio-metallurgy, the direct oxidant of pyrite is Fe^{3+} [16]. The bioleaching process of pyrite can be simply represented by Figure 1.

However, in the absence of bacteria, the oxidation of pyrite by Fe^{3+} is a very slow process. The presence of bacteria greatly accelerates the oxidation of pyrite by Fe^{3+} [17]. In bioleaching operations, attachment to mineral surface is a prerequisite for bacterial accelerated oxidation [19-21]. Attachment of leaching bacteria and formation of biofilms on mineral surfaces enhance bioleaching of pyrite and other metal sulfides [22]. Microbial EPS have been studied and discussed in many articles [23,24]. EPS play an essential role in mediating the contact between the cell and sulfide surface. Adsorption behavior of EPS on minerals is important for bacterial adhesion, which related to adsorption behavior of different components of EPS [25]. Glucuronic acid is considered in EPS [26-29] and Gehrke et al [20] and Sand et al [30] concluded that glucuronic acid and iron(III) ions play a pivotal role in primary adhesion due to an electrostatic attraction between pyrite and iron(III) complexes within the EPS. It has already been shown that the amount of glucuronic acid and complexed ferric iron in the EPS have direct implications for the efficiency of the leaching process [31]. However, understanding of the adsorption behavior on sulfide surfaces is lacking. Laskowski and Liu [32] reported that these polymers adsorb through interactions with metal-hydroxy species on the pyrite surfaces, but other adhesion mechanisms including hydrogen bonding, hydrophobic bonding, electrostatic interaction and chemical interaction have also been proposed in the literature [33,34].

In this paper, the adsorption behavior of glucuronic acid on pyrite surface was characterized using density function theory (DFT) and electrochemical methods. This paper is helpful for understanding the effect of glucuronic acid in bioleaching process.

[1] SCHOOL OF METALLURGY, NORTHEASTERN UNIVERSITY, NO. 3-11, WENHUA ROAD, HEPING DISTRICT, SHENYANG, P.R. CHINA

* Corresponding author: yanghy@smm.neu.edu.cn

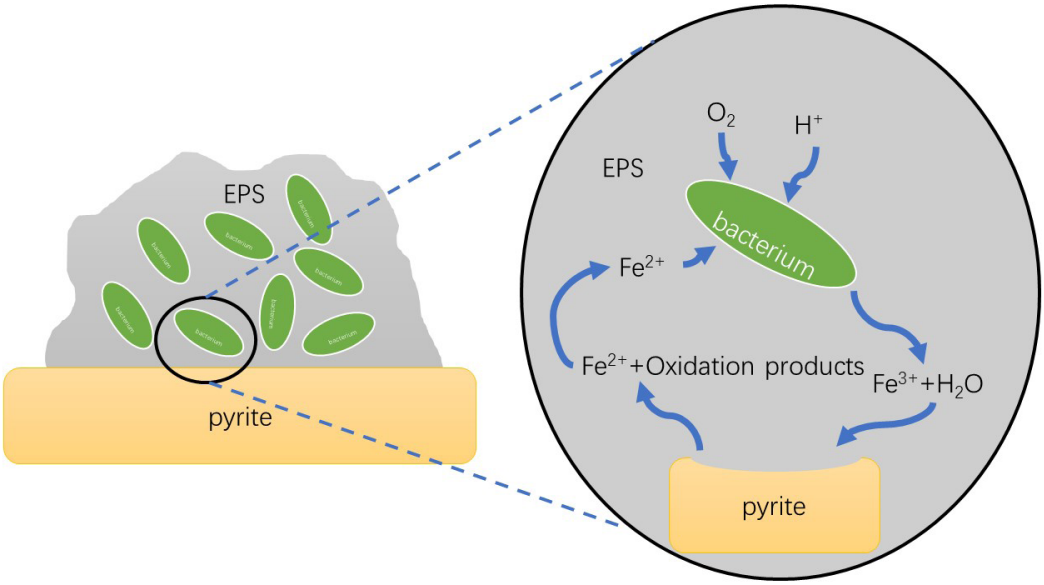

Fig. 1. Model for contact leaching catalyzed by bioleaching microorganisms

2. Experimental method

Materials

Pyrite chemical analysis was performed by combustion (sulfur) and ICP-OES (other elements) (S.C. Prospectiuni Geologice S.A.) and yielded a S:Fe atomic ratio close to 2. Main impurities detected include Si (300 mg/kg) and Al (160 mg/kg). The results of X-ray diffraction (XRD) analysis (model of the instrument: D8 ADVANCE; wavelength radiation: 1.5405 Angstrom; kV and mA values during operation: 30 KV and 40 mA; and the type of detector: LYNXEYE , Bruker Corporation, Billerica, Massachusetts, USA) of the pyrite are shown in Figure 2, which shows that the pyrite samples are pure enough for electrochemical test.

For electrochemical studies, only 1 cm^2 area was exposed during each measurement. The samples were polished using different grades of emery papers (600-1200 grade) followed by washing with ethanol, acetone and finally with distilled water before each measurement.

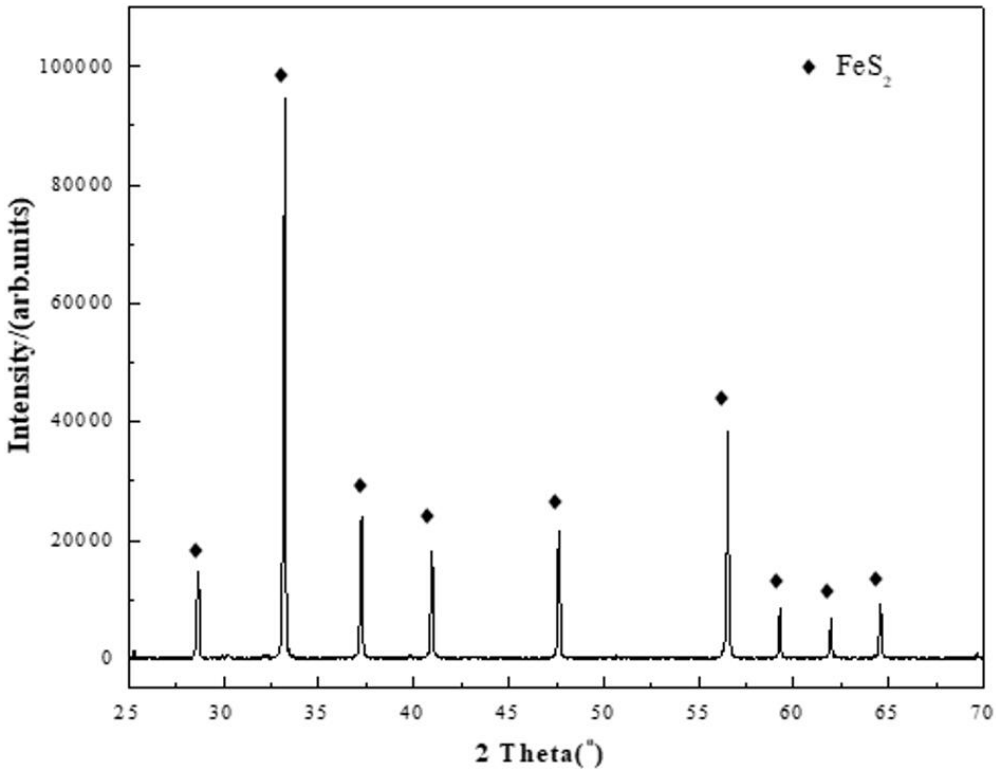

Fig. 2. The results of X-ray diffraction (XRD) analysis of the pyrite

Electrochemical experiments

Electrochemical experiments were carried out in a three-electrode cell consisting of one pyrite specimen with an exposed area of 0.185cm^2 as working electrode, a platinum counter electrode and a saturated calomel electrode (SCE) as a reference electrode. Using CH electrochemical workstation (Model No: CHI 660e, manufactured by CH Instruments, Austin, USA) at 303 K. The electrochemical experiments were carried out after 30 min to stabilize the corrosion potential of pyrite. Potentiodynamic polarization tests were conducted at the scan rate of 1.0 mV s^{-1} in the potential range from 0.2 to 0.6 V vs. SCE. Corrosion current density (i_{corr}) was obtained by Tafel extrapolation method.

DFT computational details

All calculations of DFT were performed using DMOL3 [35]. For pyrite, the Generalised Gradient Approximation (GGA) developed by J.P. Perdew, K. Burke, and M. Ernzerhof [36,37] was used to describe the exchange correlation effects. For glucuronic acid, B3LYP with electron basis set 6-31G (d, p) was used for all atoms. The geometry optimization was considered to be complete when the stationary point was located. Among the quantum parameters, Ionization potential (I) and electron afficienity (A) was calculated used E_{HOMO} and E_{LUMO} with equation (1) and (2), Several quantum chemical calculations indices, including ΔE (energy band gap), η (hardness), σ (softness), χ was the global electronegativity and ΔN was the fraction of electron transfer [38-42].

Ionization potential (I) and electron afficienity (A) was calculated using E_{HOMO} and E_{LUMO} with equation (1) and (2), Several quantum chemical calculations indices, including ΔE (energy band gap), η (hardness), σ (softness), χ is the global electronegativity and ΔN is the fraction of electron transfer [38-42]. The quantum parameters are calculated using equation (1)-(6).

$$I = -E_{HOMO} \tag{1}$$

$$A = -E_{LUMO} \tag{2}$$

$$\eta = \frac{E_{LUMO} - E_{HOMO}}{2} = \frac{\Delta E}{2} \tag{3}$$

$$\sigma = \frac{1}{\eta} \tag{4}$$

$$\chi = -\frac{1}{2}\left(E_{HOMO} + E_{LUMO}\right) \tag{5}$$

$$\Delta N = \frac{\chi_{Py} - \chi_{glo}}{2\left(\eta_{Py} + \eta_{glo}\right)} \tag{6}$$

3. Results and discussion

DFT

Adsorption behavior is closely correlated with the reactive activity of glucuronic acid and pyrite. Therefore, using GGA/BLYP/DNP method, quantum chemical parameters were calculated in aqueous phase. The results are shown in Table 1.

Band structure of pyrite is shown in Fig. 3, the band gap is 0.725eV, experimental and theoretical estimates of the pyrite (FeS_2) band gap vary from 0.73 to 1.20 eV [43-45], meaning

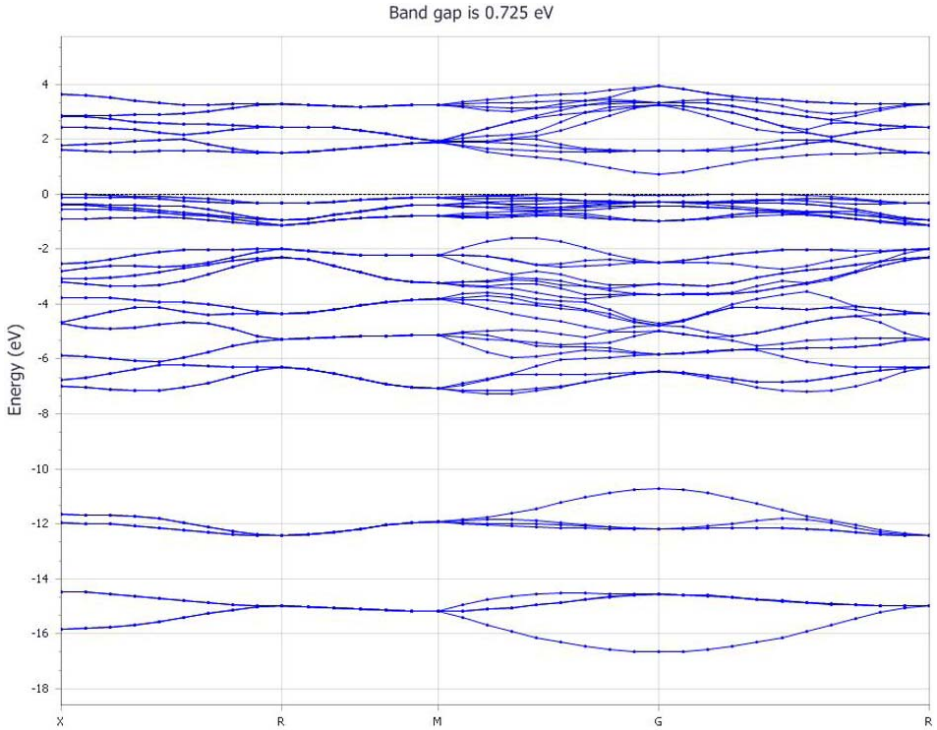

Fig. 3. Band structure of pyrite

that the results is credible. For pyrite, the value band edge is about 0.157Ha, and 0.184Ha for bottom of conduction band. Because pyrite is one type of semiconductor, we can calculate the quantum chemical calculations indices using equation (1)-(6) by value band edge and bottom of conduction band of pyrite (molecular orbit of Gamma Kpoint), which are collected in Table 1, then, the calculated indices of glucuronic acid are also listed in Table 1.

TABLE 1

Calculated indices of glucuronic acid and pyrite

Indices (Ha)	I	A	η	σ	χ	ΔN
Pyrite	0	0.027	0.014	71.429	0.014	
Glucuronic acid (liquid phase)	0.229	0.057	0.086	11.627	0.143	0.785

It is well known that any chemical reaction occurs as a result of transition of electrons due to interactions between highest occupied molecular orbital (*HOMO*) and lowest unoccupied molecular orbital (*LUMO*) of reacting species. E_{HOMO} is a quantum chemical parameter which represents the electron donating ability of the molecule. It was reported that chemical species with high values of E_{HOMO}, have the tendency to donate electrons to other chemical species with a low empty molecular orbital energy. On the contrary, the E_{LUMO} shows the ability of the molecule to accept electrons. The lower the value of E_{LUMO}, the higher its ability to accept electrons [46,47].

The *LUMO* and *HOMO* of glucuronic acid is shown in Fig. 4. The *LUMO* distribution on carboxy site of glucuronic acid, and the *HOMO* distribution concentrates on the hydroxy group of glucuronic acid. Conceding on the reducibility of pyrite surface in bio-leaching, the possible adsorption sites on pyrite surface may be the carboxy site. And Fe^{3+} may be weakly bound with hydroxy, resulting a high reaction of bioleaching. On the other hand, the, ΔN values are correlated to the adsorption efficiency resulting from electron donation, if, $\Delta N < 3.6$, the adsorption efficiency increases within creasing electron-donating ability at the minerals surface. In addition, ΔN of pyrite and glucuronic acid is –0.785, which means that glucuronic acid can capture electron from pyrite. This indicates glucuronic acid can oxidize pyrite slightly, which is consistent with the experimental results of Wang et al. [48]. This indicates that glucuronic acid and complexed ferric iron in the EPS has direct implications for the bioleaching efficiency.

Potentiodynamic polarization analysis

Potentiodynamic polarization is a useful tool to describe the relationship between electrode potential and electric current in the process of polarization. And it is widely used to obtain adsorption isotherm of organic molecules adsorbing on electrode surface, as well as to identify the effect of organic molecules on either cathodic or anodic reactions [49-52]. The polarization curves of in absence and presence of different concentration of glucuronic acid in pH 1.5 (additional sulfuric acid was added to achieve the pH) solution (the pH of bioleaching solution) are shown in Fig. 4. And Tafel data is collected in Table 2. The surface coverage (θ) is calculated using equation (7).

$$\theta = 1 - \frac{i_{corr}^{i}}{i_{corr}^{0}} \times 100\% \tag{7}$$

As we can see from Fig. 5. The shift in E_{corr} values of the different concentration of glucuronic acid compared to the acid

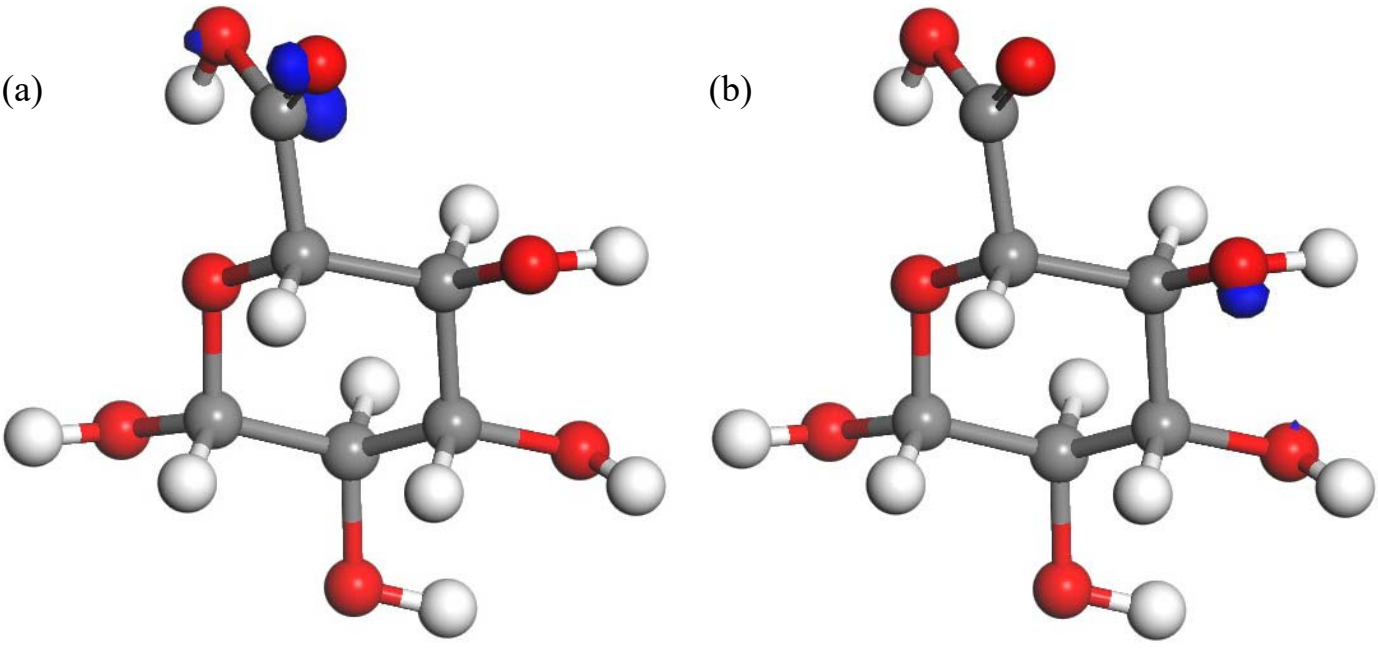

Fig. 4. *LUMO* (a) (green atmosphere) and *HOMO* (b) (green atmosphere) of glucuronic acid (isosurface value was select as 0.2) (grey ball for C atom, red ball for O atom and white ball for H atom)

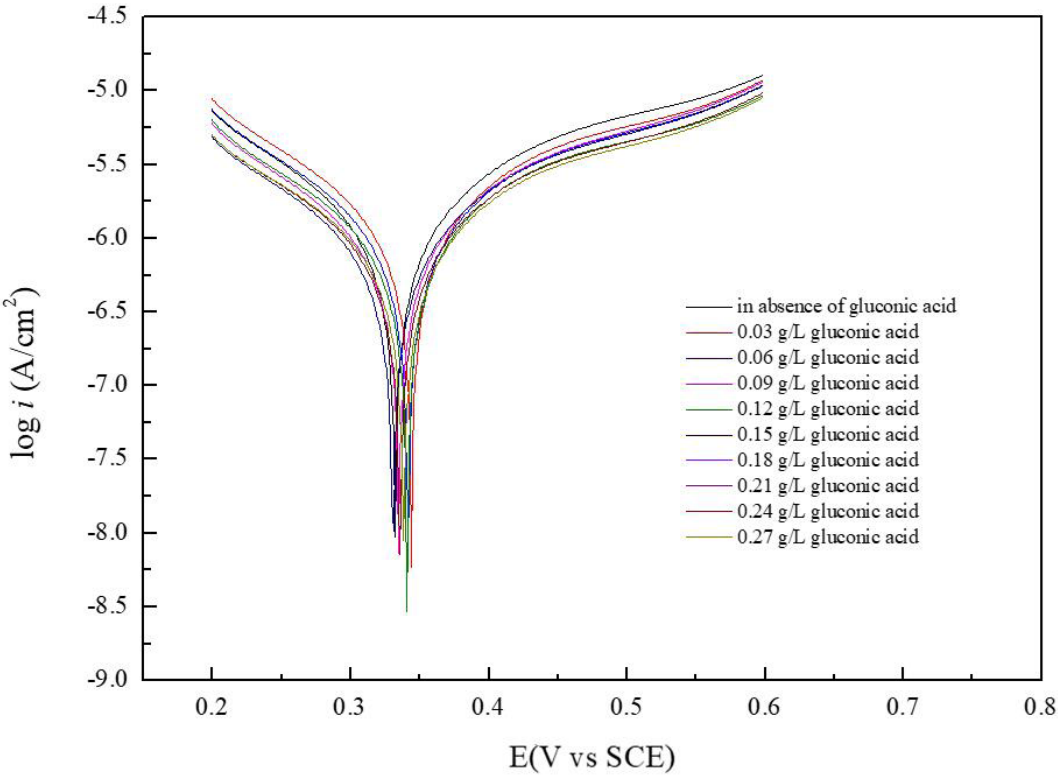

Fig. 5. The polarization curves of in absence and presence of different concentration of glucuronic acid in pH 1.5 solution

TABLE 2

Tafel data of polarization curves of in absence and presence of different concentration of glucuronic acid in pH 1.5 solution

Concentration	E_{corr} (V vs. SCE)	βc (mV Dec.$^{-1}$)	βa (mV Dec.$^{-1}$)	i_{corr} (μA cm^{-2})
0	0.344	6.611	4.458	2.296
0.03	0.346	6.275	4.636	1.962
0.06	0.349	6.105	6.506	1.705
0.09	0.343	6.436	4.699	1.508
0.12	0.342	6.323	4.671	1.346
0.15	0.335	6.449	5.019	1.141
0.18	0.337	6.169	4.839	1.118
0.21	0.331	6.316	5.316	1.065
0.24	0.336	6.129	4.860	1.055
0.27	0.338	6.004	4.800	1.048

blank is less than 80 mV, suggesting that the studied surfactants are mixed type inhibitors (with the effect of adsorption) [53,54]. The values of both anodic and cathodic Tafel slopes (βc, βa) slightly changed when the concentration of the gluconic acid increased, which suggests that the addition of the gluconic reduces the anodic dissolution of pyrite (without Fe^{3+} in the solution) as well as effects of the cathodic reaction, without affecting the reactions mechanism. The decreases of the corresponding current densities and the increase in the degree of surface coverage (θ) with increasing glucuronic acid concentration due to the formation of anodic protective films on the electrode surface [55].

Adsorption isotherm

Adsorption behavior can be described by adsorption isotherm, i.e. as those given by the Frumkin, Langmuir, and Temkin models, among others [56], which can give key information of adsorption. The adsorption isotherm is shown in Fig 6. Using Langmuir model to fit the data, R^2 is 0.982, which indicates that the adsorption isotherm can be described as Langmuir isotherm. We can also describe Langmuir isotherm by Equation (8)

$$\frac{C}{\theta} = \frac{1}{k_{ads}} + C \tag{8}$$

where C is the concentration of glucuronic acid, k the adsorptive equilibrium constant and θ is the surface coverage. The adsorption isotherm was determined from the polarization curves after 30 min of immersion. The adsorption equilibrium constant k_{ads} is 1.276×10^3,which reflects the high adsorption ability of glucuronic acid on the pyrite surface.

Standard free energy of adsorption is related to k_{ads} according to the following equation (3). $\Delta G_{ads}{}^0 = -RTln(55.5k_{ads})$ Equation (3) where R J mol^{-1} K^{-1} is the universal gas constant and T (K) is the absolute temperature and 55.5 mol L^{-1} is the molar concentration of water in solution. $\Delta G_{ads}{}^0$ is calculated to be –27.67 kJ mol^{-1}, the negative value means the spontaneity of the adsorption of glucuronic acid on pyrite surface and the stabile adsorbed layer on pyrite surface, as well as the strong interaction of glucuronic acid and pyrite surface. Generally, absolute values of $\Delta G_{ads}{}^0$ around 20 kJ mol^{-1} or less negative are consistent with electrostatic interactions between inhibitor and the charged

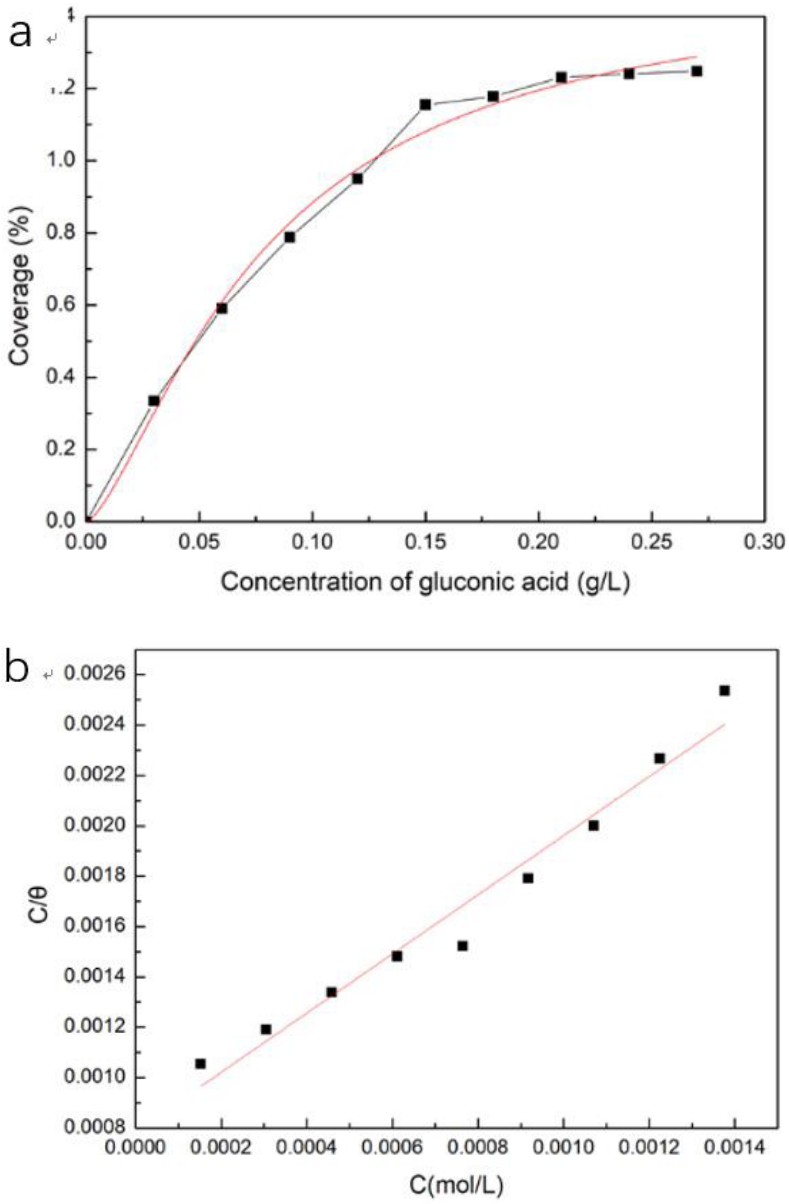

Fig. 6. The adsorption isotherm of gluconic on pyrite; (a) Fitting with concentration and coverage; (b) Fitting with concentration (C) and C/θ

metal surface (physisorption), while those around 40 kJ mol^{-1} or higher are associated with chemisorption as a result of the sharing or transfer of electrons from organic molecules to the surface to form a coordinate type of bonds (chemisorption) [25]. Accordingly, the value of ΔG_{ads}^{0}, –27.67 kJ mol^{-1} suggests that the adsorption of glucuronic acid on the pyrite surface takes place through both chemical and physical adsorption.

4. Conclusion

In the present study, adsorption behavior of glucuronic acid on pyrite surface was investigated by DFT and electrochemical methods. Following conclusions are drawn:

1. Adsorption capacity of glucuronic acid is stronger than that of water, in water solution, glucuronic acid tends to absorb on pyrite surface.
2. Electrons transfer from pyrite to glucuronic acid when glucuronic acid adsorbs on pyrite surface. Glucuronic acid can oxidize pyrite slightly.
3. Adsorption of glucuronic acid on pyrite surface follows Langmuir's adsorption isotherm with adsorption standard free energy of –27.67 kJ mol^{-1}.
4. Glucuronic acid adsorbs on pyrite surface by mixed type interactions (physisorption and chemisorption).

Acknowledgement

Projects (U1608254,51374066) supported by the National Natural Science Foundation of China; Assistance of Material Studio is supported by pro. JianHua Chen from GuangXi University.

REFERENCES

[1] T. Gu, S.O. Rastegar, S.M. Mousavi, M. Li, M. Zhou, Advances in bioleaching for recovery of metals and bioremediation of fuel ash and sewage sludge, Bioresource Technol. **261**, 428-440 (2018).

[2] S. Ghosh, S. Mohanty, A. Akcil, L.B. Sukla, A.P. Das, A greener approach for resource recycling: Manganese bioleaching, Chemosphere **154**, 628-639 (2016).

[3] Y. Konishi, S. Asai, M. Tokushige, T. Suzuki, Bioleaching of chalcopyrite concentrate by acidophilic thermophile Acidianus brierleyi, Biotechnol. Progr. **15**, 681-688 (2010).

[4] T.-J. Peng, Z. Dan, X.-D. Liu, R.-L. Yu, T. Jiang, G.-H. Gu, C. Miao, G.-Z. Qiu, W.-M. Zeng, Enrichment of ferric iron on mineral surface during bioleaching of chalcopyrite, T. Nonferr. Metal. Soc. **26**, 544-550 (2016).

[5] L. Ma, X. Wang, X. Liu, S. Wang, H. Wang, Intensified bioleaching of chalcopyrite by communities with enriched ferrous or sulfur oxidizers, Bioresource Technol. **268**, 415-423 (2018).

[6] D. Shin, J. Jeong, S. Lee, B.D. Pandey, J.C. Lee, Evaluation of bioleaching factors on gold recovery from ore by cyanide-producing bacteria, Miner. Eng. **48**, 20-24 (2013).

[7] J.-L. Xia, J.J. Song, H.-C. Liu, Z.-Y. Nie, L. Shen, P. Yuan, C.-Y. Ma, L. Zheng, Y.-D. Zhao, Study on catalytic mechanism of silver ions in bioleaching of chalcopyrite by SR-XRD and XANES, Hydrometallurgy **180**, 26-35 (2018).

[8] J.V. Mehrabani, S.Z. Shafaei, M. Noaparast, S.M. Mousavi, Bioleaching of high pyrite carbon-rich sphalerite preflotation tailings, Environ. Earth. Sci. **71**, 4675-4682 (2014).

[9] Y. Huai, C. Plackowski, Y. Peng, The surface properties of pyrite coupled with gold in the presence of oxygen, Miner. Eng. **111**, 131-139 (2017).

[10] C. Lü, Y. Wang, P. Qian, Y. Liu, G. Fu, J. Ding, S. Ye, Y. Chen, Separation of chalcopyrite and pyrite from a copper tailing by ammonium humate, Chinese. J. Chem. Eng. **26**, 1814-1821 (2018).

[11] M. Ejtemaei, A.V. Nguyen, Characterisation of sphalerite and pyrite surfaces activated by copper sulphate, Miner. Eng. **100**, 223-232 (2017).

[12] Y. Huai, C. Plackowski, Y. Peng, The galvanic interaction between gold and pyrite in the presence of ferric ions, Miner. Eng. **119**, 236-243 (2018).

[13] F. Estrada-de los Santos, R. Rivera-Santillán, M. Talavera-Ortega, F. Bautista, Catalytic and galvanic effects of pyrite on ferric leaching of sphalerite, Hydrometallurgy **163**, 167-175 (2016).

[14] Y. Morishita, N. Shimada, K. Shimada, Invisible gold in arsenian pyrite from the high-grade Hishikari gold deposit, Japan: Significance of variation and distribution of Au/As ratios in pyrite, Ore. Geol. Rev. **95**, 79-93 (2018).

[15] E. Bidari, V. Aghazadeh, Pyrite from Zarshuran Carlin-type gold deposit: Characterization, alkaline oxidation pretreatment, and cyanidation, Hydrometallurgy **179**, 222-231 (2018).

[16] W. Sand, T. Gehrke, Extracellular polymeric substances mediate bioleaching/biocorrosion via interfacial processes involving iron (III) ions and acidophilic bacteria, Res. Microbiol. **157**, 49-56 (2006).

[17] J.N. Xu, H.Y. Yang, Electrochemical Research on N-Type and P-Type Semiconductor Pyrite, Adv. Mater. Res. **1130**, 179-182 (2015).

[18] S. Barahona, C. Dorador, R. Zhang, P. Aguilar, W. Sand, M. Vera, F. Remonsellez, Isolation and characterization of a novel Acidithiobacillus ferrivorans strain from the Chilean Altiplano: attachment and biofilm formation on pyrite at low temperature, Res. Microbiol **165**, 782-793 (2014).

[19] S. Bellenberg, M. Díaz, N. Noël, W. Sand, A. Poetsch, N. Guiliani, M. Vera, Biofilm formation, communication and interactions of leaching bacteria during colonization of pyrite and sulfur surfaces, Res. Microbiol. **165**, 773-781 (2014).

[20] T. Gehrke, J. Telegdi, D. Thierry, W. Sand, Importance of Extracellular Polymeric Substances from Thiobacillus ferrooxidans for Bioleaching, Appl. Environ. Microbiol. **64**, 2743-2747 (1998).

[21] L.X. Yan, W.D. Zhou, Z.L. Xi, Function of Bacterial Attachment on the Pre-Biooxidation of Arsenic-Bearing Gold Concentrate, Journal of Northeastern University **21**, 641-644 (2000).

[22] B. Florian, N. Noël, W. Sand, S.T.L. Harrison, J. Petersen, R.P.V. Hille, Visualization of initial attachment of bioleaching bacteria using combined atomic force and epifluorescence microscopy, Miner. Eng. **23**, 532-535 (2010).

[23] H.E. Zhi-Guo, Y.P. Yang, S. Zhou, H.U. Yue-Hua, H. Zhong, Effect of pyrite, elemental sulfur and ferrous ions on EPS production by metal sulfide bioleaching microbes, T. Nonferr. Metal. Soc. **24**, 1171-1178 (2014).

[24] Q. Li, W. Sand, Mechanical and chemical studies on EPS from Sulfobacillus thermosulfidooxidans: from planktonic to biofilm cells, Colloids & Surfaces B Biointerfaces **153**, 34-40 (2017).

[25] C.A. Jerez, Bioleaching and Biomining for the Industrial Recovery of Metals, 2017, Elsevier, Chile.

[26] Z. Wang, X. Xie, S. Xiao, J. Liu, Adsorption behavior of glucose on pyrite surface investigated by TG, FTIR and XRD analyses, Hydrometallurgy **102**, 87-90 (2010).

[27] J. Zhu, Q. Li, W. Jiao, H. Jiang, W. Sand, J. Xia, X. Liu, W. Qin, G. Qiu, Y. Hu, Adhesion forces between cells of Acidithiobacillus ferrooxidans, Acidithiobacillus thiooxidans or Leptospirillum ferrooxidans and chalcopyrite, Colloids & Surfaces B Biointerfaces **94**, 95 (2012).

[28] R. Zhang, S. Bellenberg, L. Castro, T.R. Neu, W. Sand, M. Vera, Colonization and biofilm formation of the extremely acidophilic archaeon Ferroplasma acidiphilum, Hydrometallurgy **150**, 245-252 (2014).

[29] Q. Li, W. Sand, R. Zhang, Enhancement of Biofilm Formation on Pyrite by Sulfobacillus thermosulfidooxidans, Minerals **6**, 71 (2016).

[30] S. Bellenberg, C.F. Leon-Morales, W. Sand, M. Vera, Visualization of capsular polysaccharide induction in Acidithiobacillus ferrooxidans, Hydrometallurgy **129-130**, 82-89 (2012).

[31] W. Sand, T. Gehrke, Extracellular polymeric substances mediate bioleaching/biocorrosion via interfacial processes involving iron(III) ions and acidophilic bacteria, Res. Microbiol. **157**, 49 (2006).

[32] K. Harneit, A. Göksel, D. Kock, J.H. Klock, T. Gehrke, W. Sand, Adhesion to metal sulfide surfaces by cells of Acidithiobacillus

ferrooxidans, Acidithiobacillus thiooxidans and Leptospirillum ferrooxidans, Hydrometallurgy **83**, 245-254 (2006).

[33] Q. Liu, Y. Zhang, J.S. Laskowski, The adsorption of polysaccharides onto mineral surfaces: an acid/base interaction, Int. J. Miner. Process. **60**, 229-245 (2000).

[34] E. Bogusz, S.R. Brienne, I. Butler, S.R. Rao, J.A. Finch, Metal ions and dextrin adsorption on pyrite, Miner. Eng. **10**, 441-445 (1997).

[35] Y. Li, Q. Liu, Adsorption behaviour and interaction mechanisms of dextrin on oxidative mineral surface, T. Nonferr. Metal. Soc. **6**, 30-33 (1996).

[36] B. Delley, From molecules to solids with the DMol3 approach, J. Chem. Phys. **113**, 7756-7764 (2000)

[37] J.P. Perdew, K. Burke, M. Ernzerhof, Generalized Gradient Approximation Made Simple, Physical Review Letters **77**, 3865-3868 (1996).

[38] Y. Xian, Y. Wang, S. Wen, Q. Nie, J. Deng, Floatability and oxidation of pyrite with different spatial symmetry, Miner. Eng. **72**, 94-100 (2015).

[39] T. Arslan, F. Kandemirli, E.E. Ebenso, I. Love, H. Alemu, Quantum chemical studies on the corrosion inhibition of some sulphonamides on mild steel in acidic medium, Corros. Sci. **51**, 35-47 (2009).

[40] J. Cruz, R. MartíNez, J. Genesca, E. GarcíA-Ochoa, Experimental and theoretical study of 1-(2-ethylamino)-2-methylimidazoline as an inhibitor of carbon steel corrosion in acid media, J. Electroanal. Chem. **566**, 111-121 (2004).

[41] H. Ju, Z.P. Kai, Y. Li, Aminic nitrogen-bearing polydentate Schiff base compounds as corrosion inhibitors for iron in acidic media: A quantum chemical calculation, Corros. Sci. **50**, 865-871 (2008).

[42] G. Gao, C. Liang, Electrochemical and DFT studies of β-aminoalcohols as corrosion inhibitors for brass, Electrochim. Acta **52**, 4554-4559 (2007).

[43] I.B. Obot, N.O. Obi-Egbedi, Theoretical study of benzimidazole and its derivatives and their potential activity as corrosion inhibitors, Corros. Sci. **52**, 657-660 (2010).

[44] S. Khalid, M.A. Malik, D.J. Lewis, P. Kevin, E. Ahmed, Y. Khan, P. O'Brien, Transition Metal Doped Pyrite (FeS2) Thin Films: Structural Properties and Evaluation of Optical Band Gap Energies, Journal of Materials Chemistry C **3**, 12068-12076 (2015).

[45] J. Hu, Y. Zhang, M. Law, R. Wu, Increasing the Band Gap of Iron Pyrite by Alloying with Oxygen, J. Am. Chem. Soc. **134**, 13216-13219 (2016).

[46] M. Blanchard, M. Alfredsson, J. Brodholt et al., Arsenic incorporation into FeS_2, pyrite and its influence on dissolution: A DFT study, Geochimica et Cosmochimica. Acta **71**, 624-630 (2007).

[47] I.B. Obot, S. Kaya, C. Kaya, B. Tüzün, Density Functional Theory (DFT) modeling and Monte Carlo simulation assessment of inhibition performance of some carbohydrazide Schiff bases for steel corrosion, Physica. E **80**, 82-90 (2016).

[48] Z.H. Wang, L.U. Jian-Jun, L.U. Xian-Cai, L.I. Juan, The effects of the typical components of extracellular polymeric substances(EPS) of microorganism on the bio-decomposition of pyrite, Acta Petrologica et Miner. **28**, 553-558 (2009).

[49] L.H. Madkour, Correlation between corrosion inhibitive effect and quantum molecular structure of Schiff bases for iron in acidic and alkaline media, Nature **2**, 680-704 (2014).

[50] M. Yadav, D. Sharma, T.K. Sarkar, Adsorption and corrosion inhibitive properties of synthesized hydrazine compounds on N80 steel/hydrochloric acid interface: Electrochemical and DFT studies, J. Mol. Liq. **212**, 451-460 (2015).

[51] H. Lgaz, V. Srivastava, J. Haque, C. Verma, P. Singh, R. Salghi, M.A. Quraishi, Amino acid based imidazolium zwitterions as novel and green corrosion inhibitors for mild steel: Experimental, DFT and MD studies, J. Mol. Liq. **244**, 340-352 (2017).

[52] S. Benabid, T. Douadi, S. Issaadi, C. Penverne, S. Chafaa, Electrochemical and DFT studies of a new synthesized Schiff base as corrosion inhibitor in 1M HCl, Measurement **59**, 53-63 (2016).

[53] J.H. Al-Fahemi, M. Abdallah, E.A.M. Gad, Experimental and theoretical approach studies for melatonin drug as safely corrosion inhibitors for carbon steel using DFT, J. Mol. Liq. **222**, 1157-1163 (2016).

[54] W. Xiao, L. Liang, W. Pan, L. Wen, J. Zhang, Y. Yan, How the Inhibition Performance Is Affected by Inhibitor Concentration: A Perspective from Microscopic Adsorption Behavior, Ind. Eng. Chem. Res. **53**, 16785-16792 (2014).

[55] M.A. Bedair, M.M.B. El-Sabbah, A.S. Fouda, H.M. Elaryian, Synthesis, electrochemical and quantum chemical studies of some prepared surfactants based on azodye and Schiff base as corrosion inhibitors for steel in acid medium, Corros. Sci. **128**, 54-72 (2017).

[56] J. Aldana-González, A. Espinoza-Vázquez, M. Romero-Romo, J. Uruchurtu-Chavarin, M. Palomar-Pardavé, Electrochemical evaluation of cephalothin as corrosion inhibitor for API 5L X52 steel immersed in an acid medium, Arab. J. Chem. **11**, 0903-0903 (2015).

[57] A. Espinoza-Vázquez, G.E. Negrón-Silva, R. González-Olvera, D. Angeles-Beltrán, H. Herrera-Hernández, M. Romero-Romo, M. Palomar-Pardavé, Mild steel corrosion inhibition in HCl by di-alkyl and di-1,2,3-triazole derivatives of uracil and thymine, Mater. Chem. Phys. **145**, 407-417 (2014).